Supporting Information

The Sensitivity of Cu for Electrochemical Carbon Dioxide Reduction to Hydrocarbons as Revealed by High Throughput Experiments

Yungchieh Lai[1], Ryan J.R. Jones[1], Yu Wang[1], Lan Zhou[1], Matthias H. Richter[1], and John Gregoire[1]

[1] Joint Center for Artificial Photosynthesis, California Institute of Technology, Pasadena, CA 91024

[*] gregoire@caltech.edu

Material Synthesis

Cu thin film electrocatalysts were fabricated using DC magnetron sputtering of a 2" Cu metal target at 50 W in 6 mTorr Ar onto a 100 mm-diameter Si wafer with an approximately 170 nm SiO2 diffusion barrier and 10 nm Ti adhesion layer, using a previously described sputter system with 10-5 Pa base pressure.1 After deposition, the films were stored in a nitrogen purge box until the day of electrochemical testing, although no other catalyst treatment was performed prior to electrocatalyst screening. The Cu-X (X: Co, Sn, Zn, Al, Mn, In, Ni, Sb) thin film electrodes were deposited under similar conditions from elemental metal targets with DC power adjusted to obtain designed composition in the wafer center. All the metal targets were pre-cleaned in the presence of 6 mTorr Ar for 10 min to remove any contaminants from the target surface. The non-confocal geometry of sputter source provided a continuous composition gradient across the Si wafer with the composition variation within each 5 mm-diameter electrode being less than 1% for the most Cu-rich catalysts and about 2% for the most Cu-poor catalysts.

Electrochemistry

ECMS

Electrochemical mass spectrometry (ECMS) was previously published for rapid CO_2RR electrocatalyst screening.[1] Prior to the electrolysis, the electrolyte (0.1 M $KHCO_3$, >=99.95% trace metals basis, Sigma Aldrich) was purged with CO_2 (99.999%, Airgas) for at least 30 min. A bipolar membrane (BPM, Fumasep® FBM single film, Fumatech) was used to separate the working and counter electrodes. Platinum wire (99.9%, Sigma Aldrich) was used as the counter electrode. The surface area of the counter electrode was ca. 0.25 cm^2, while the working electrode surface area was 0.32 cm^2.

Electrolysis was carried out with a Gamry Reference 600TM potentiostat. All electrochemical data were collected using a Ag/AgCl reference electrode (LF2, Innovative Instruments) and converted to a reversible hydrogen electrode (RHE) scale using the measured solution pH of 6.8 The uncompensated solution resistance was measured by performing electrochemical impedance spectroscopy (EIS) in the frequency range of 100 Hz–500 kHz with an amplitude of 10 mV at the open circuit potential of a Cu-Pt working electrode-counter electrode system. The uncompensated resistance, R_u, was measured by using a Nyquist plot of the EIS spectra and was found to be 60 Ω. All electrochemical measurements are compensated by this value in post-processing to yield figures with resistance-compensated values of electrochemical potential. For each composition of the library, 3 cycles of cyclic voltammetry (CV) at 10mV/s was scanned from -0.4 to -1.3 (V) vs RHE (resistance uncompensated). Open circuit potential for 1 minutes was conducted in between each CV cycle for mass spectrometer signal to return to baseline. The flow rate of electrolyte was 160 μL/s throughout the tests and the reaction product generated was

carried by the electrolyte to the downstream evaporator to collect the product for detection by mass spectrometer.

Mass spectra were acquired on a Hiden HPR20 mass spectrometer connected to the outlet of the dessicant chamber. An electron energy of 70 eV was used for ionization of all species, with an emission current of 20 μA. Hydrogen (m/z = 2), methane (m/z = 15), ethylene (m/z = 26) ions were accelerated with a voltage of 3 V. All mass-selected product cations were detected by a secondary electron multiplier with a detector voltage of 940 V. The dwell and settle time were set at 25% to optimize for speed and a data point was recorded every ca. 12.5 s.

ANEC

Analytical and Electro-chemistry (ANEC) is an analytical electrochemistry system previously published by our group that can efficiently detects a wide range of CO_2RR product.[2] This system is applied in this study to further explore those Cu-X catalysts that are rpresentative of the primary conclusions. Prior to the electrolysis, the electrolyte 0.1 M $KHCO_3$ Potassium bicarbonate (>= 99.95% trace metals basis) was purged with CO_2 (99.999%, Airgas) for at least 30 min. A bipolar membrane (Fumasep® FBM single film, Fumatech) was used to separate the working and counter electrodes. Platinum wire (99.9%, Sigma Aldrich) was used as the counter electrode. The surface area of the counter electrode was about 0.25 cm^2, while the working electrode surface area was 0.32 cm^2.

Electrolysis was carried out with a Gamry Reference 600™ potentiostat. The uncompensated solution resistance was measured by performing electrochemical impedance spectroscopy (EIS) in the frequency range of 100Hz to 500kHz with an amplitude of 10 mV at the open circuit potential of a Pt-Pt Working Electrode-Counter Electrode system. The uncompensated resistance, R_u, was measured by using a Nyquist plot of the EIS spectra and was found to be 72 Ohms. All electrochemical data was collected *vs.* a Ag/AgCl reference electrode (LF2, Innovative Instruments) and converted to a reversible hydrogen electrode (RHE) scale. For each composition of the library, 4 sequential electrolyses were performed: (a) 15 min CP at -3 mA/cm^2, (b) 15 min CP at -1 mA/cm^2, (c) 4.5 min CP at -10 mA/cm^2, and (d) 15 min CP at -3 mA/cm^2. The first electrolysis was considered to be a pretreatment for the catalyst and the last three electrolyses were used as the reported results. At the end of each electrolysis, gaseous and liquid products were sampled by the robotic sample handling system (RSHS) and analyzed by GC (Thermo Scientific™ TRACE™ 1300) and HPLC (Thermo Scientific UltiMate 3000). The cell and all solution handling lines are purged with fresh electrolyte and CO_2 between electrolysis to avoid cross-contamination.

H-cell

A PEEK compression cell (Fig. S1) was used as the vessel for the H-cell measurement in a three-electrode configuration with anode and cathode chamber volumes of 2 mL, and counter and working electrode area of 1 cm 2 and a 2.4 cm 2 membrane. 0.1 M potassium bicarbonate ($KHCO_3$) buffer (pH 6.8) was used as the electrolyte. The corresponding anion exchange

membrane (AEM) was Selemion. Pt foil was used as the counter electrode and a leakless Ag/AgCl reference electrode. All electrochemical measurements were performed using a Biologic VSP-300 potentiostats. Gas flow rates of the flow controller (Gas inlet) and flow meter (Gas outlet) where recorded by the external device inputs of the potentiostat.

The electrochemical setup was operated in a continuous flow mode. Humidified carbon dioxide was provided to the electrochemical cell and its flow rate was controlled with an Alicat flow controller (5 sccm, gas bubbler between cell and flow controller). The exhaust gasses went through a liquid trap than an Alicat flow meter and finally to a gas chromatograph (SRI-8610) using a Hayesep D column with N_2 as the carrier gas. The gaseous products were detected using a thermal conductivity detector (TCD) and flame ionization detector (FID) equipped with a methanizer. Quantitative analysis of gaseous products was based on calibration with several gas standards over many orders of magnitude in concentration.

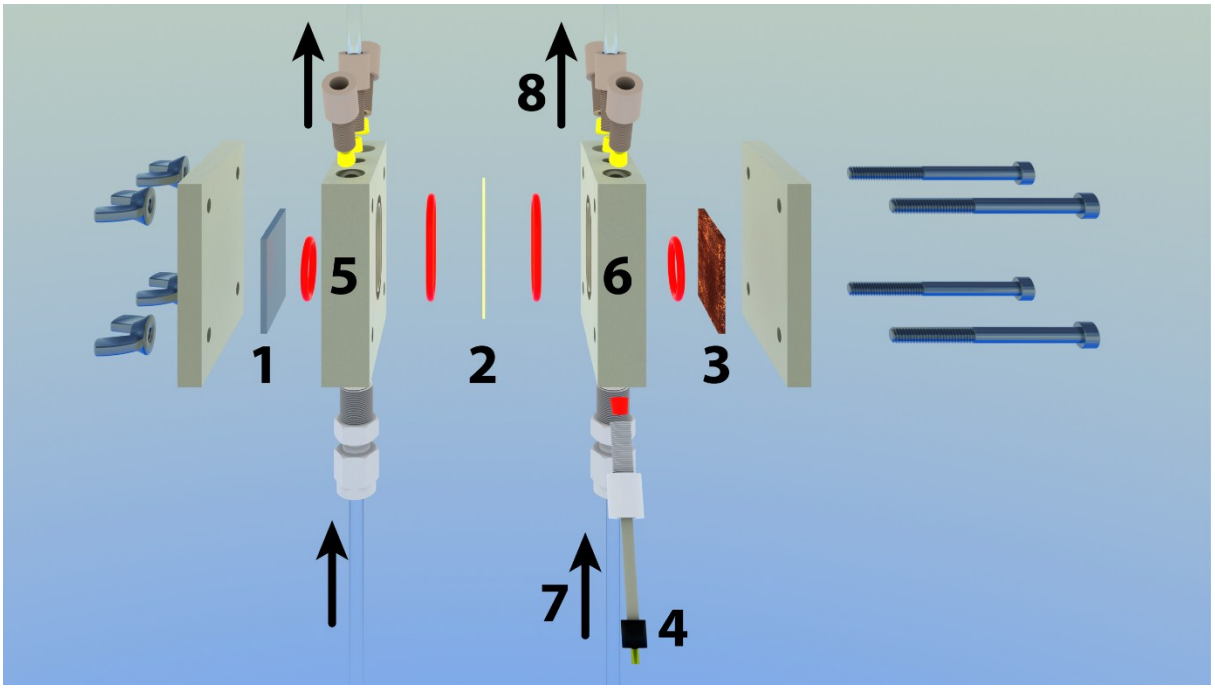

Figure S1. Compression H-cell configuration composed of 1 Pt counter electrode, 2 anion exchange membrane, 3 sample under test, 4 ref electrode, 5 anolyte chamber, 6 catholyte chamber, 7 gas inlet, and 8 gas outlet. Black arrows indicate the gas flow.

Material Characterization

The bulk composition of the Cu-X alloys were characterized via x-ray fluorescence (XRF, EDAX Orbis MicroXRF). The synchrotron measurements were performed at beamline 1−5 of the Stanford Synchrotron Radiation Light source (SSRL) at SLAC National Accelerator Laboratory using a 12.7 keV source in reflection scattering geometry with a setup described previously.[3] The composition of all the alloys screened is shown in table S1.

Table S1. Compositions of Cu-X alloys screened in this reported work.

Sample #	Cu (%)							
	CuCo	CuSn	CuZn	CuAl	CuMn	CuIn	CuNi	CuSb
1	98.3	99	98.9	99.45	98.7	98.9	98.6	99
2	97.8	98.1	98.3	98.9	98	98.4	98	98.6
3	96.7	96.9	97.4	98.2	97	97.7	96.8	97.2
4	94.8	95.3	96.1	96.5	95.6	96.5	95.2	95.7
5	92	91.5	93.7	92.9	93	94.7	93	93.5
6	88.3	86.2	91	88.1	88	90	90	89
7	83.5	78.2	87.3	79	85.8	87.9	85.1	86.6
8	76	--	85.3	74	81	84	81	83

X-ray photoelectron spectroscopy (XPS) was used to investigate surface composition of Cu-X alloys synthesized for CO_2RR. XPS data were collected using a Kratos Axis Nova system with a base pressure of ~1×10^{-9} Torr equipped with a monochromatic AlKα X-ray source with a photon energy of 1486.6 eV. Photoelectrons were collected at 0° from the surface normal with a retarding pass energy of 160 eV for survey XPS scans (step size 1.0 eV) and 20 eV for high-resolution core levels scans (step size 0.05 eV). Both alloys were measured on multiple spots to assure meaningful statistics.

Validation studies for Cu-Sb, Cu-In, and Cu-Mn

To demonstrate the trends observed from this fast ECMS technique is transferrable, a few follow up tests were operated by other analytical electrochemistry systems including ANEC.[2] Similar to conventional H-cell, ANEC can detect wide range of CO_2RR product by passing products from electrochemical cell into both GC and HPLC. In contrast to conventional cells, however, product including the gas ones was recirculated within the ANEC electrochemical cell to quickly accumulate concentration. The accumulation of product enable detection by analytical instrument within short-duration electrochemistry and hence increases throughput.

As discussed, Cu-Sb and Cu-In shows lower selectivity toward hydrogen and high "other product" charge. Results of CuSb tested by this technique is shown in Fig S15 and S16. It confirms the qualitative trends from ECMS (Fig S15) and provides quantitative detection of the products that cannot be detected by ECMS (Fig S16). Specifically, selectivity to methane drops significantly but not that to ethylene at low Sb concentration (i.e. ~ 2 at. %). Selectivity to liquid product including formic acid and alcohol was also suppressed. The decreases in FE of these products corresponds to an increase in FE of CO. At higher Sb concentration, hydrocarbons and alcohols are substantially suppressed, and hydrogen evolution reaction (HER) slightly decreases which is accompanied with increased selectivity of CO at more positive potentials. Conventional H-cell was further used to confirm above observations and is shown in Fig S17, with excellent qualitative agreement and some quantitative differences that are likely the result of different mass transport conditions in the different cells. The result of Cu-In is shown in Fig S18. ANEC again confirms the qualitative trends from ECMS and shows what the "other product" is in Fig 4. Interestingly, the suppressed hydrogen and hydrocarbons turns out to become significantly increased CO formation, up to FE > 80% at In ~2%.

ANEC results for Cu-Mn are shown in Fig S20 and confirm the observations from ECMS that the product distribution is less sensitive to Mn than to In, Sb, etc., with the most substantial difference being a drop in the relative CH_4 concentration. This is most pronounced in the 4.4% Mn sample where FE for CH_4 is substantially lowered while the C_2 products are relatively unchanged or increase slightly in FE. Further investigation will be required to see whether the presence of Mn improves C-C coupling, or whether the surface Mn occupies Cu sites that would otherwise be selective for CH_4.

Note that above results show only major product with FE > 1%.

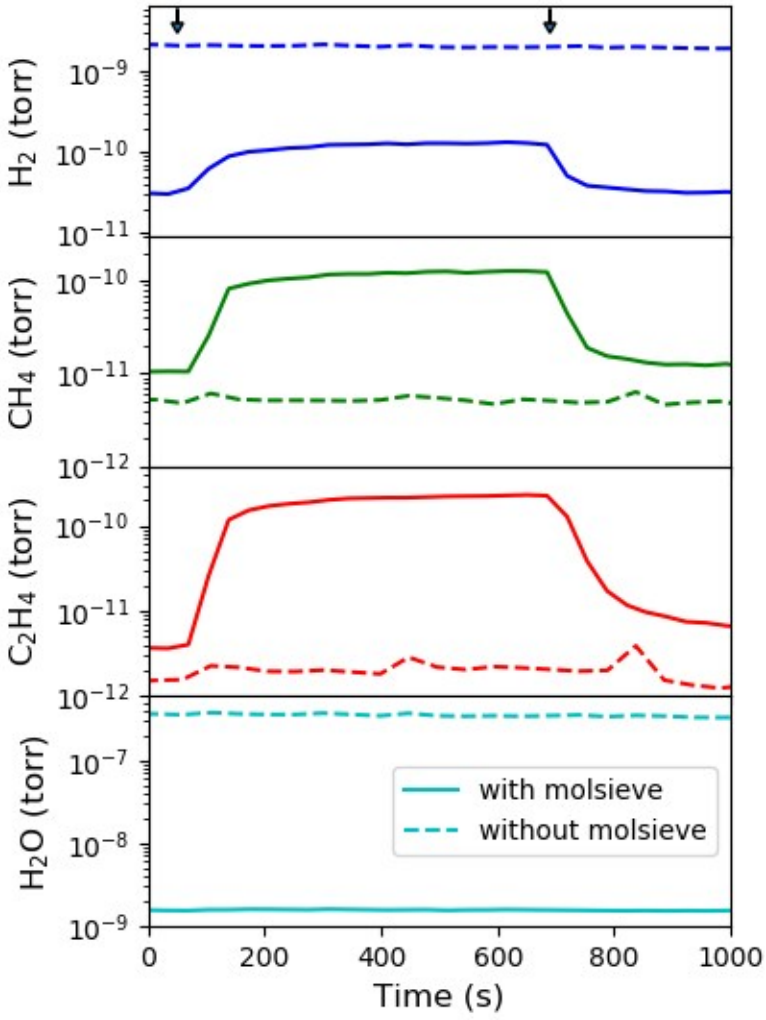

Figure S2. MS signal comparison between with and without mol. sieve applied in the EC-MS system. The comparison was made by controlling the total MS pressure to be ~1.5 μTorr for each test. The first arrow on the left indicates when the flowing electrolyte was switched from CO_2-bubbled one to

calibration gas-bubbled one, while the arrow on the right indicates a reversed switch. The calibration gas used for bubbling electrolyte is consisted of 1% H_2, 1% CH_4, and 1% C_2H_4 balanced with CO_2.

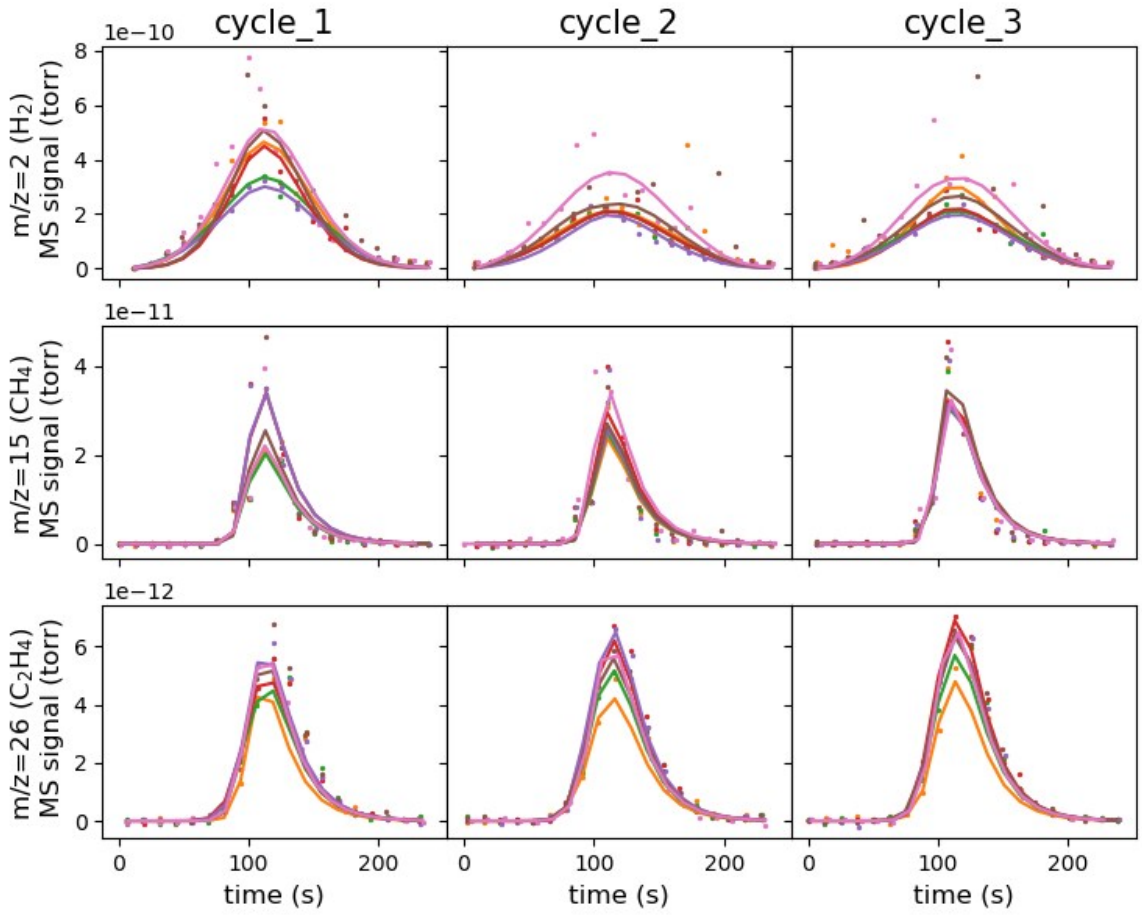

Figure S3. Raw (dotted line) and fitted MS signal (solid line) for 3CVs scanned sequentially over 6 Cu thin film electrodes.

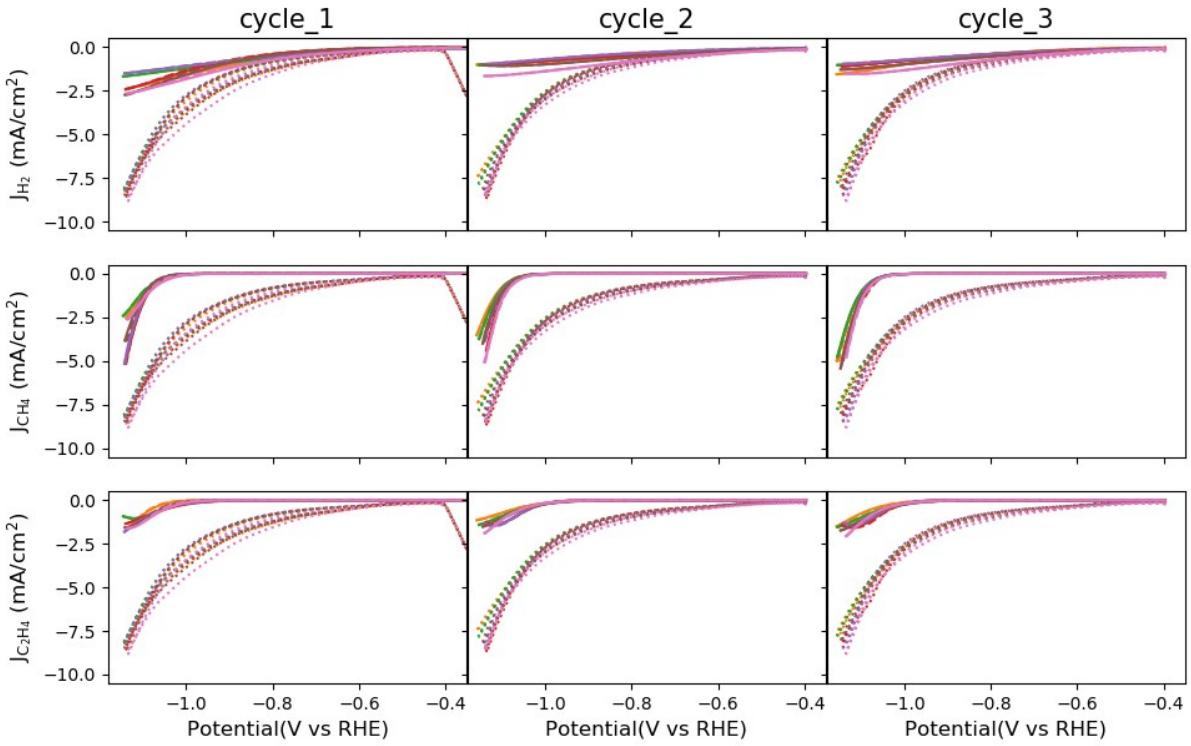

Figure S4. Smoothed Jtotal (dotted line, same data for each product) and modeled Jp (solid line for cathodic sweep and dashed line for anodic sweep, although strong overlap with cathodic sweep makes anodic and cathodic indistinguishable) for 3 CVs scanned sequentially over 6 Cu thin film electrodes.

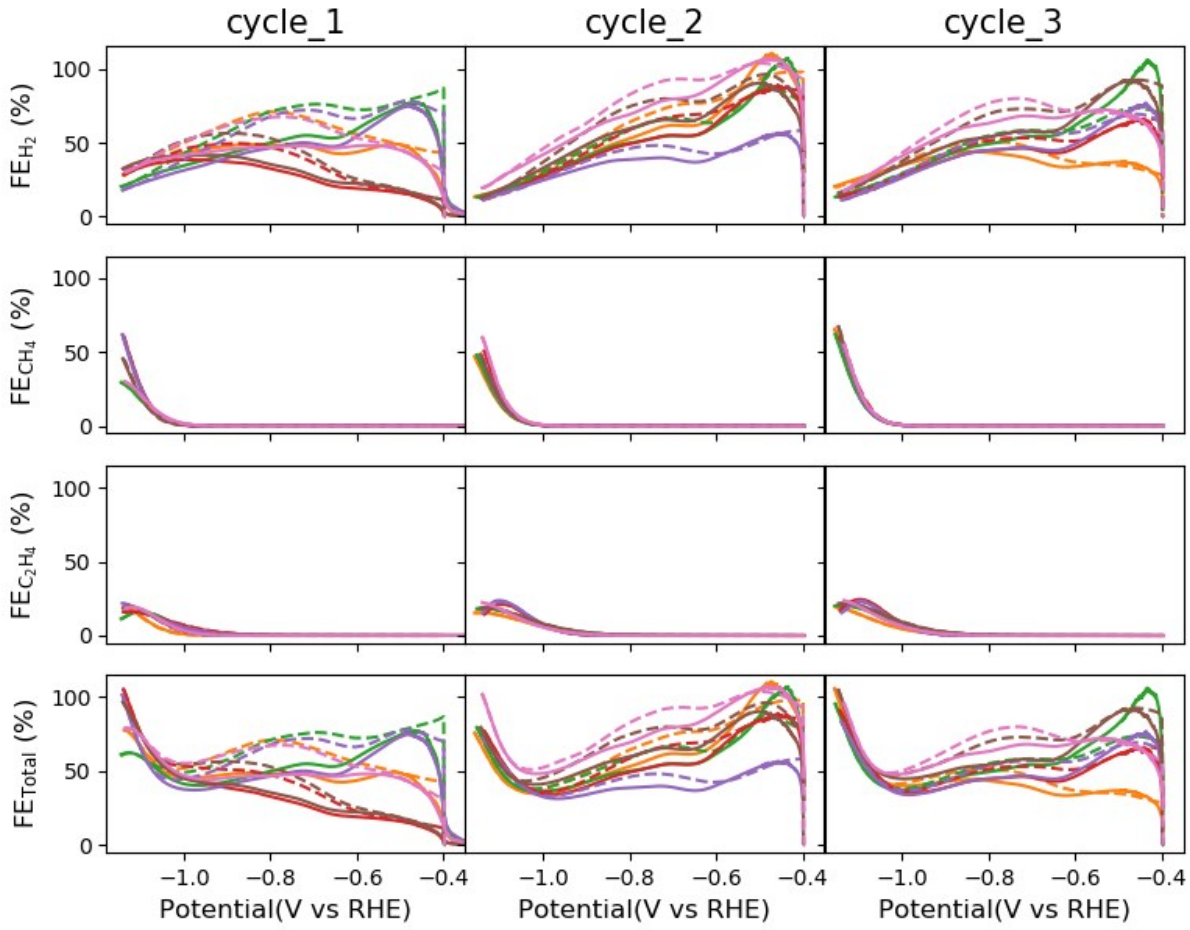

Figure S5. FE (solid line for cathodic sweep and dashed line for anodic sweep) for 3 CVs scanned sequentially over 6 Cu thin film electrodes.

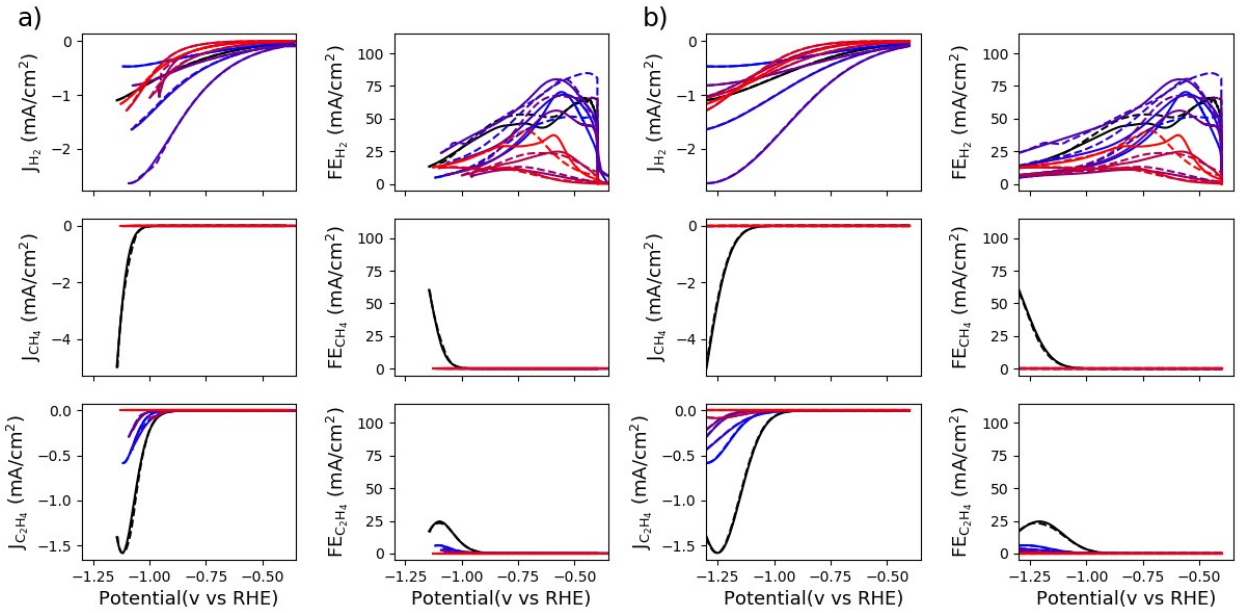

Figure S6. Modeled Jp and FE for 3rd-cycle CuSb test. Potential was a) with and b) without resistance compensated. Color from blue to red indicates concentration of secondary metal increases from sample spot 1 to 8 and black curve is the referenced Cu. Solid line: modeled cathodic Jp/FE; dashed line: modeled anodic Jp/FE; dotted line: smoothed measured current.

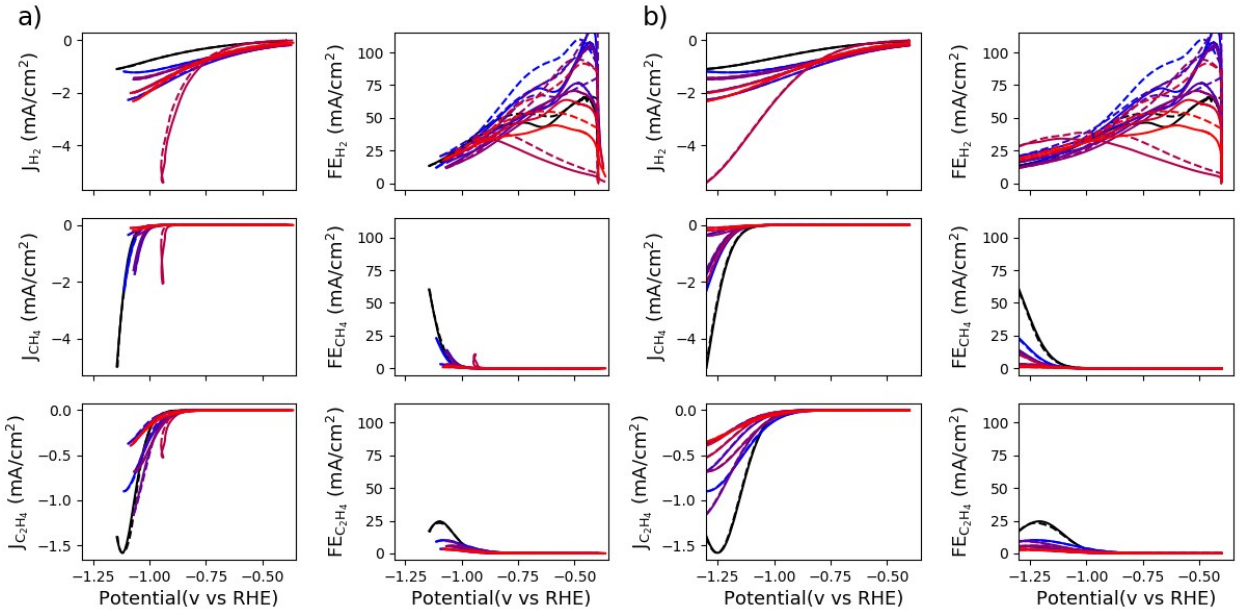

Figure S7. Modeled Jp and FE for 3rd-cycle CuNi test. Potential was a) with and b) without resistance compensated. Color from blue to red indicates concentration of secondary metal increases from sample spot 1 to 8 and black curve is the referenced Cu. Solid line: modeled cathodic Jp/FE; dashed line: modeled anodic Jp/FE; dotted line: smoothed measured current.

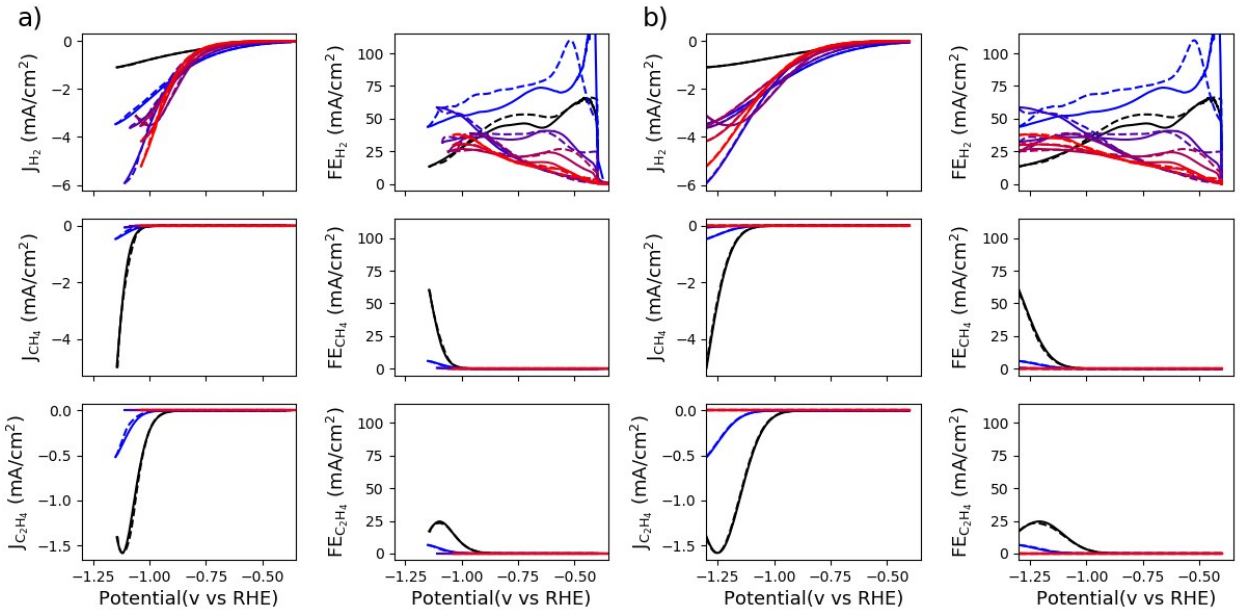

Figure S8. Modeled Jp and FE for 3rd-cycle CuIn test. Potential was a) with and b) without resistance compensated. Color from blue to red indicates concentration of secondary metal increases from sample spot 1 to 7 and black curve is the referenced Cu. Solid line: modeled cathodic Jp/FE; dashed line: modeled anodic Jp/FE; dotted line: smoothed measured current.

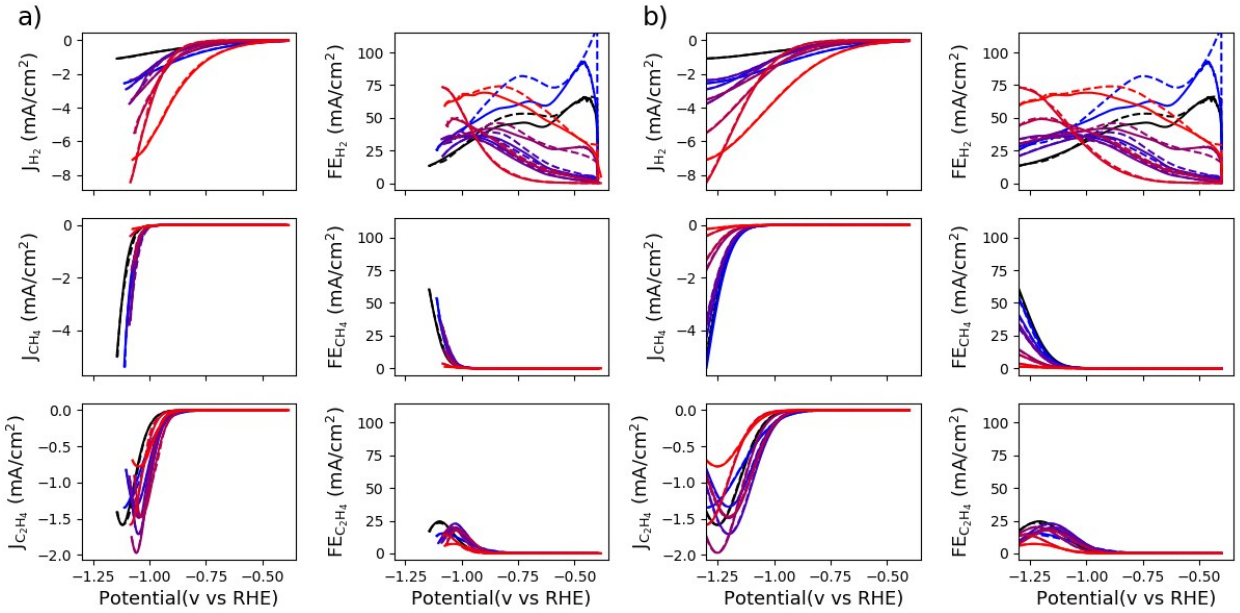

Figure S9. Modeled Jp and FE for 3rd-cycle CuMn test. Potential was a) with and b) without resistance compensated. C Color from blue to red indicates concentration of secondary metal increases from sample spot 1 to 8 and black curve is the referenced Cu. Solid line: modeled cathodic Jp/FE; dashed line: modeled anodic Jp/FE; dotted line: smoothed measured current.

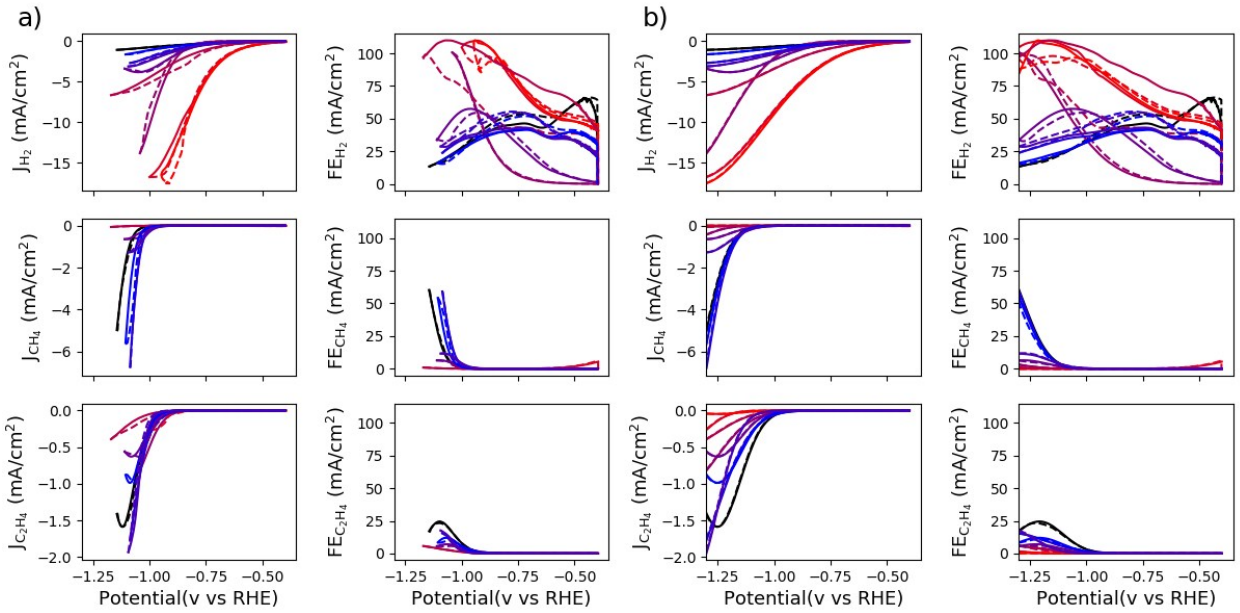

Figure S10. Modeled Jp and FE for 3rd-cycle CuAl test. Potential was a) with and b) without resistance compensated. Color from blue to red indicates concentration of secondary metal increases from sample spot 1 to 8 and black curve is the referenced Cu. Solid line: modeled cathodic Jp/FE; dashed line: modeled anodic Jp/FE; dotted line: smoothed measured current.

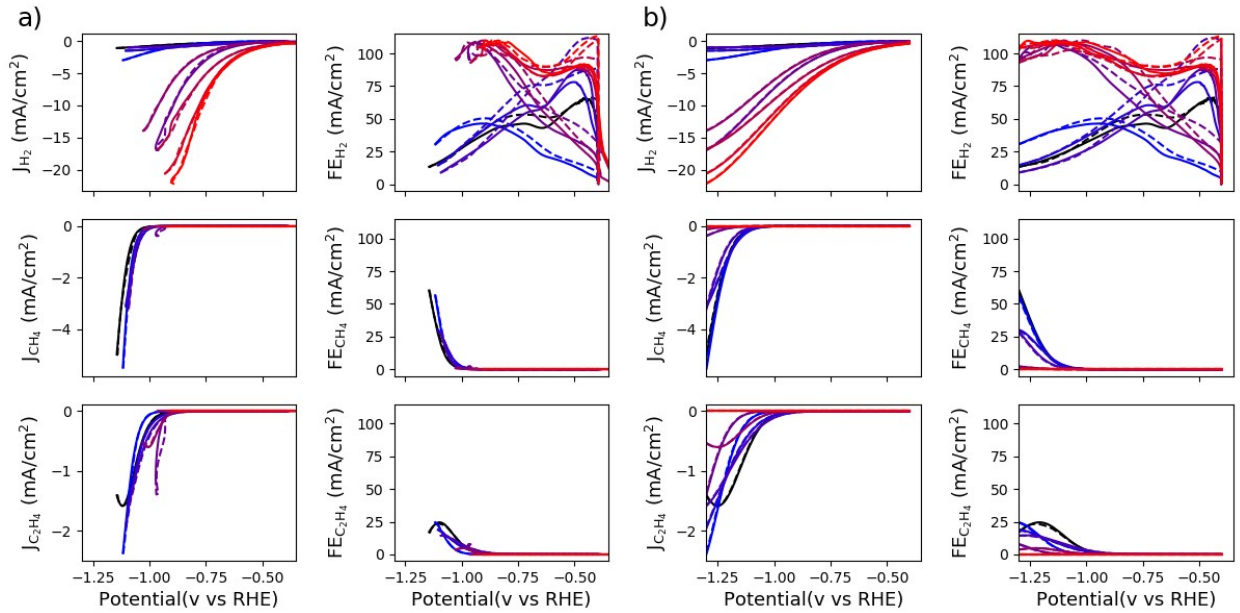

Figure S11. Modeled Jp and FE for 3rd-cycle CuZn test. Potential was a) with and b) without resistance compensated. Color from blue to red indicates concentration of secondary metal increases from sample spot 1 to 8 and black curve is the referenced Cu. Solid line: modeled cathodic Jp/FE; dashed line: modeled anodic Jp/FE; dotted line: smoothed measured current.

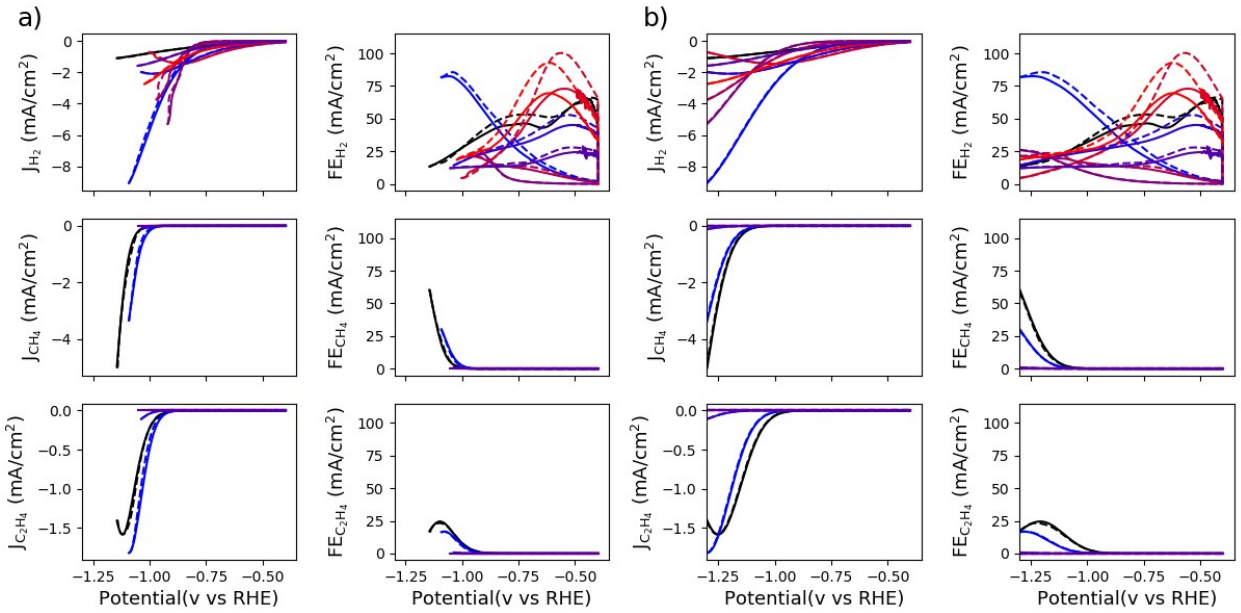

Figure S12. Modeled Jp and FE for 3rd-cycle CuSn test. Potential was a) with and b) without resistance compensated. Color from blue to red indicates concentration of secondary metal increases from sample spot 1 to 7 and black curve is the referenced Cu. Solid line: modeled cathodic Jp/FE; dashed line: modeled anodic Jp/FE; dotted line: smoothed measured current.

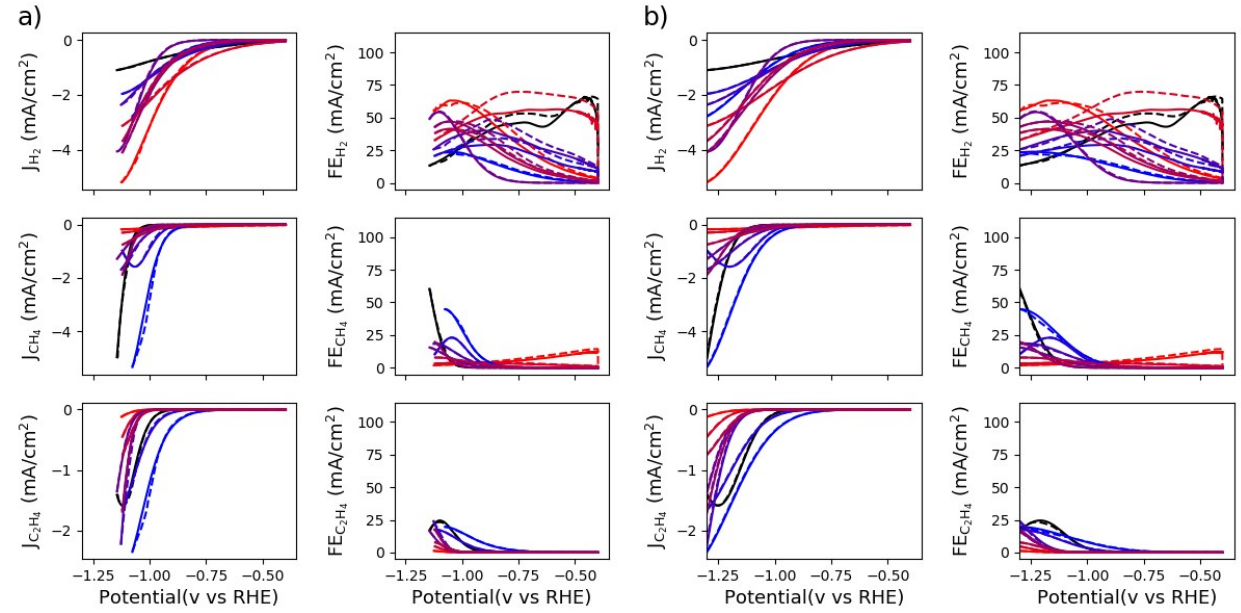

Figure S13. Modeled Jp and FE for 3rd-cycle CuCo test. Potential was a) with and b) without resistance compensated. Color from blue to red indicates concentration of secondary metal increases from sample spot 1 to 8 and black curve is the referenced Cu. Solid line: modeled cathodic Jp/FE; dashed line: modeled anodic Jp/FE; dotted line: smoothed measured current.

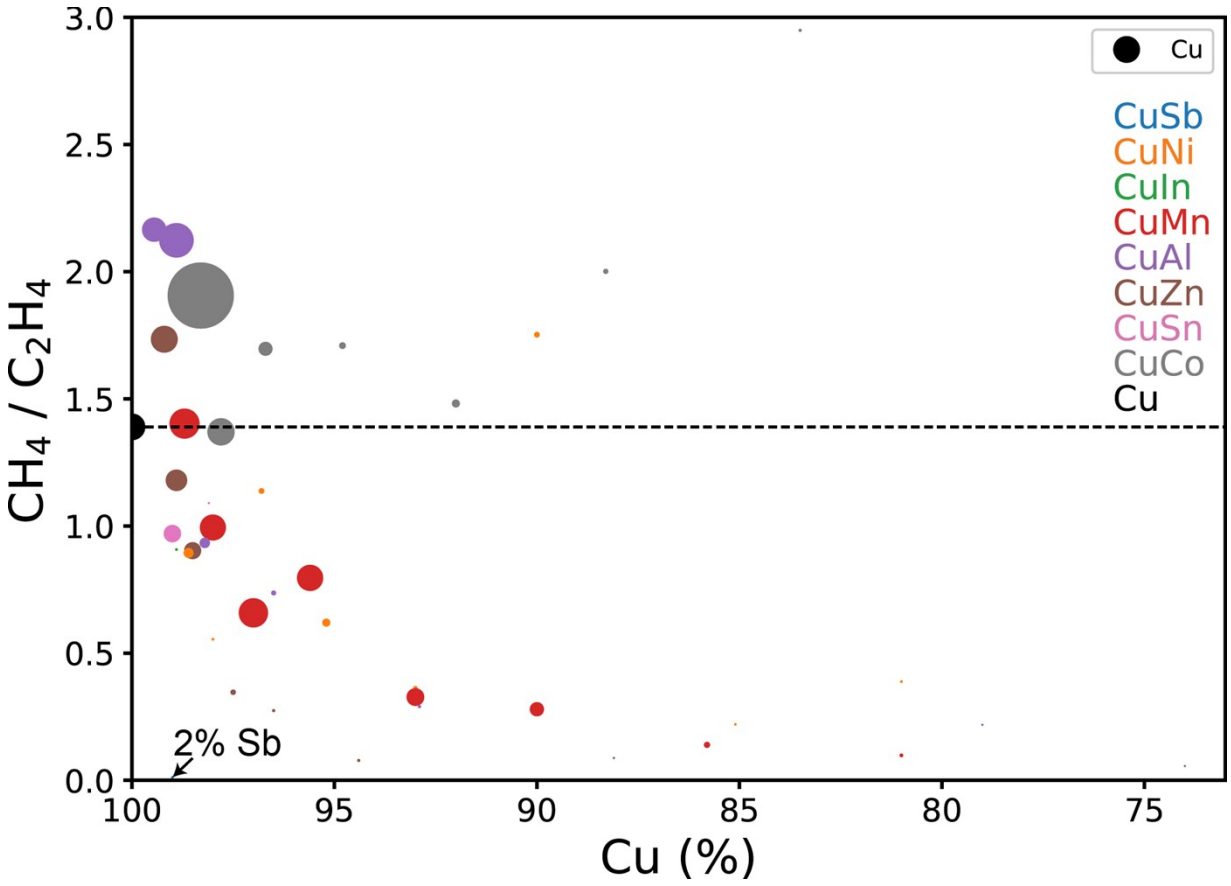

Figure S14. CH_4 to C_2H_4 ratio for the 8 Cu alloy tested. The marker size was determined by dividing HC formation of Cu-alloys to that of Cu film

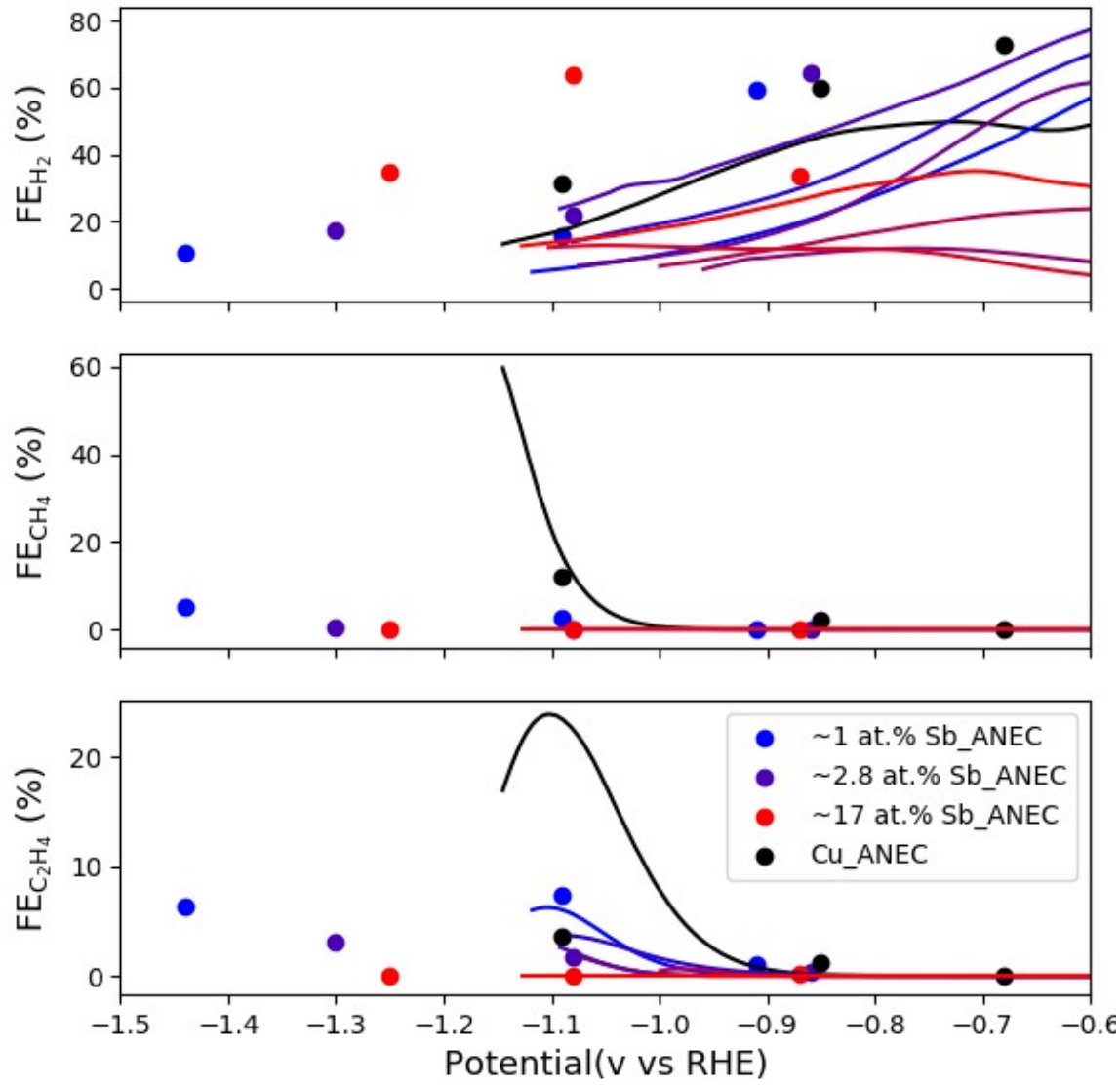

Figure S15. Cu-Sb gas product distribution comparison between ECMS and ANEC. Blue to red indicates alloys ranging from less Sb-rich to more Sb-rich. The solid lines are results from the averaged signal of cathodic and anodic sweep from ECMS shown in figure S6. Note that Sb concentration indicated here is nominal and may vary up to 2 at. % between the tests by ECMS and ANEC due to the location difference on binary plate library

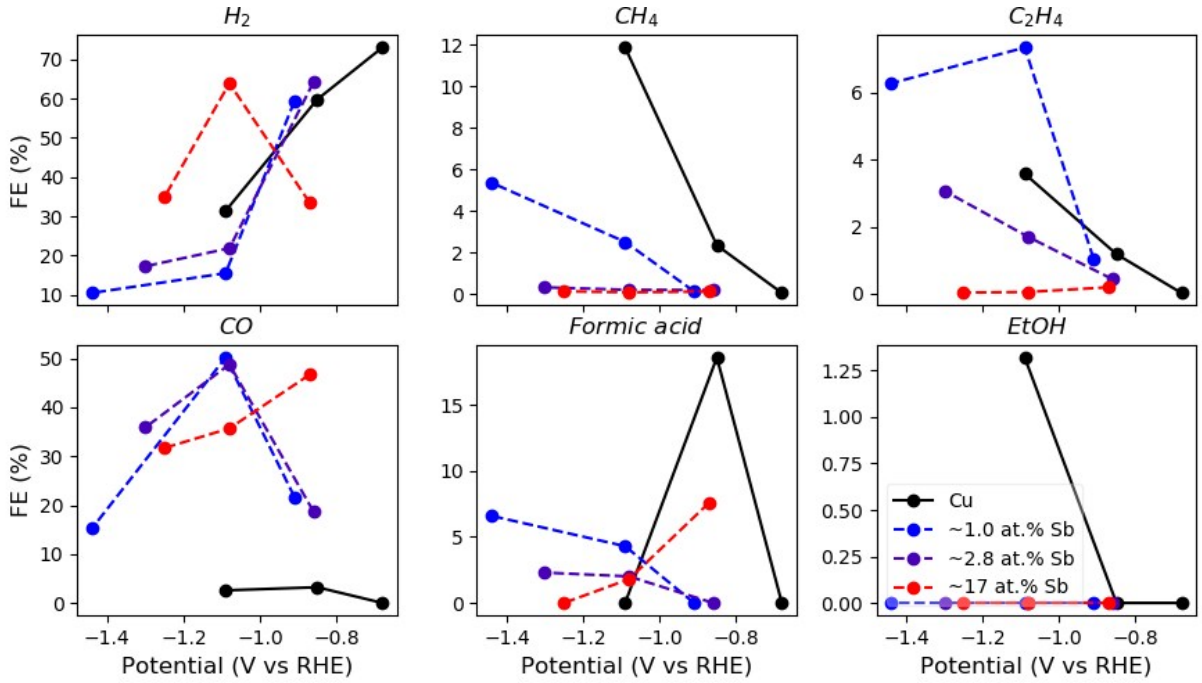

Figure S16. Product distribution of Cu-Sb including liquid product analyzed by ANEC. Note that Sb concentration indicated here is nominal and may vary up to 2 at. % between the tests by ECMS and ANEC due to the location difference on binary plate library

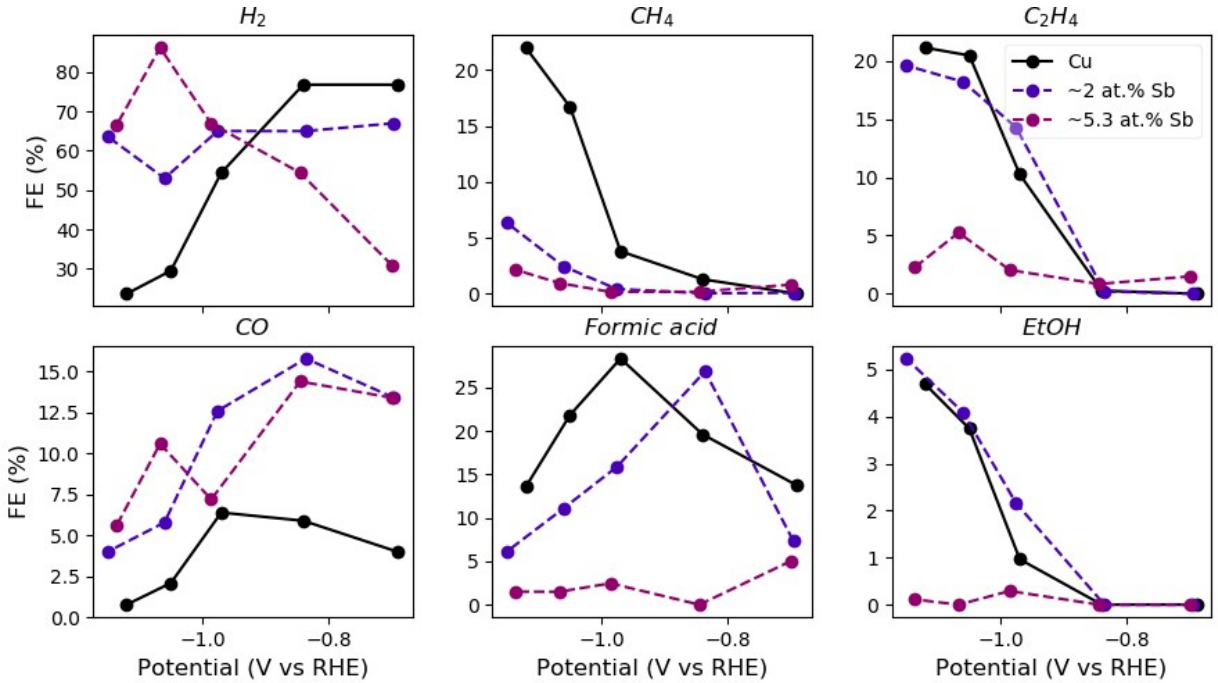

Figure S17. Product distribution of Cu-Sb analyzed by H-cell. Note that Sb concentration indicated here is nominal and may vary up to 4 at. % between the tests by H-cell and other cells due to the location and the tested area differences on binary plate library

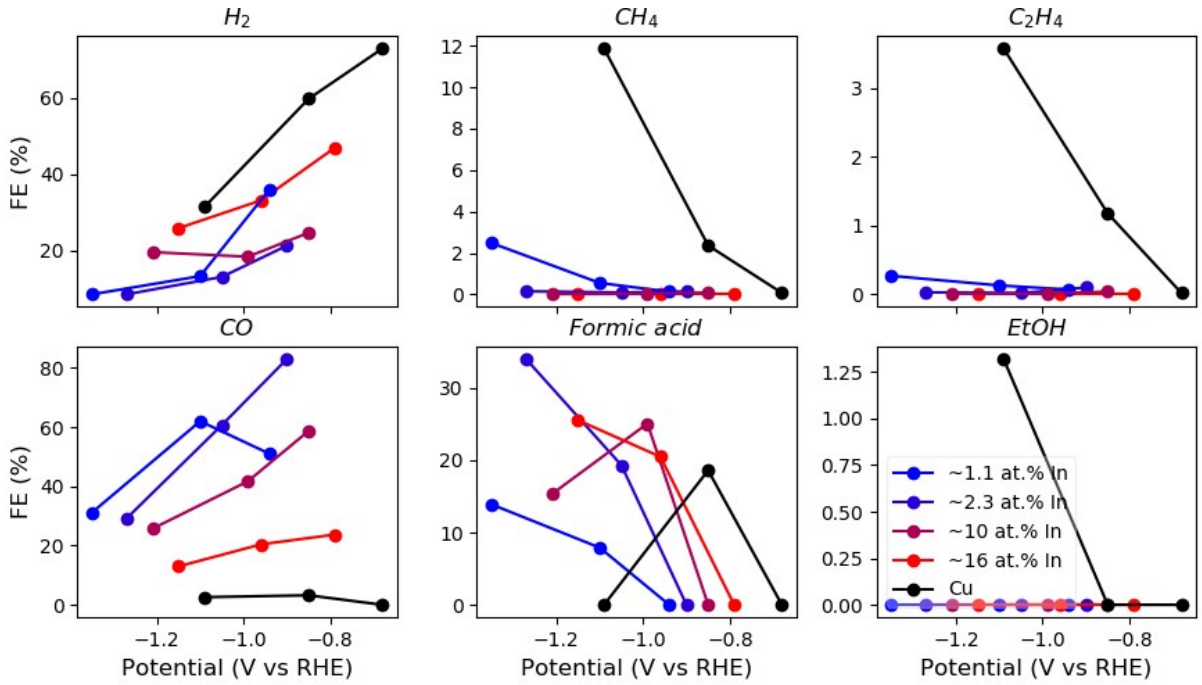

Figure S18. Product distribution of Cu-In including liquid product analyzed by ANEC. Note that In concentration indicated here is nominal and may vary up to 2 at. % between the tests by ECMS and ANEC due to the location difference on binary plate library

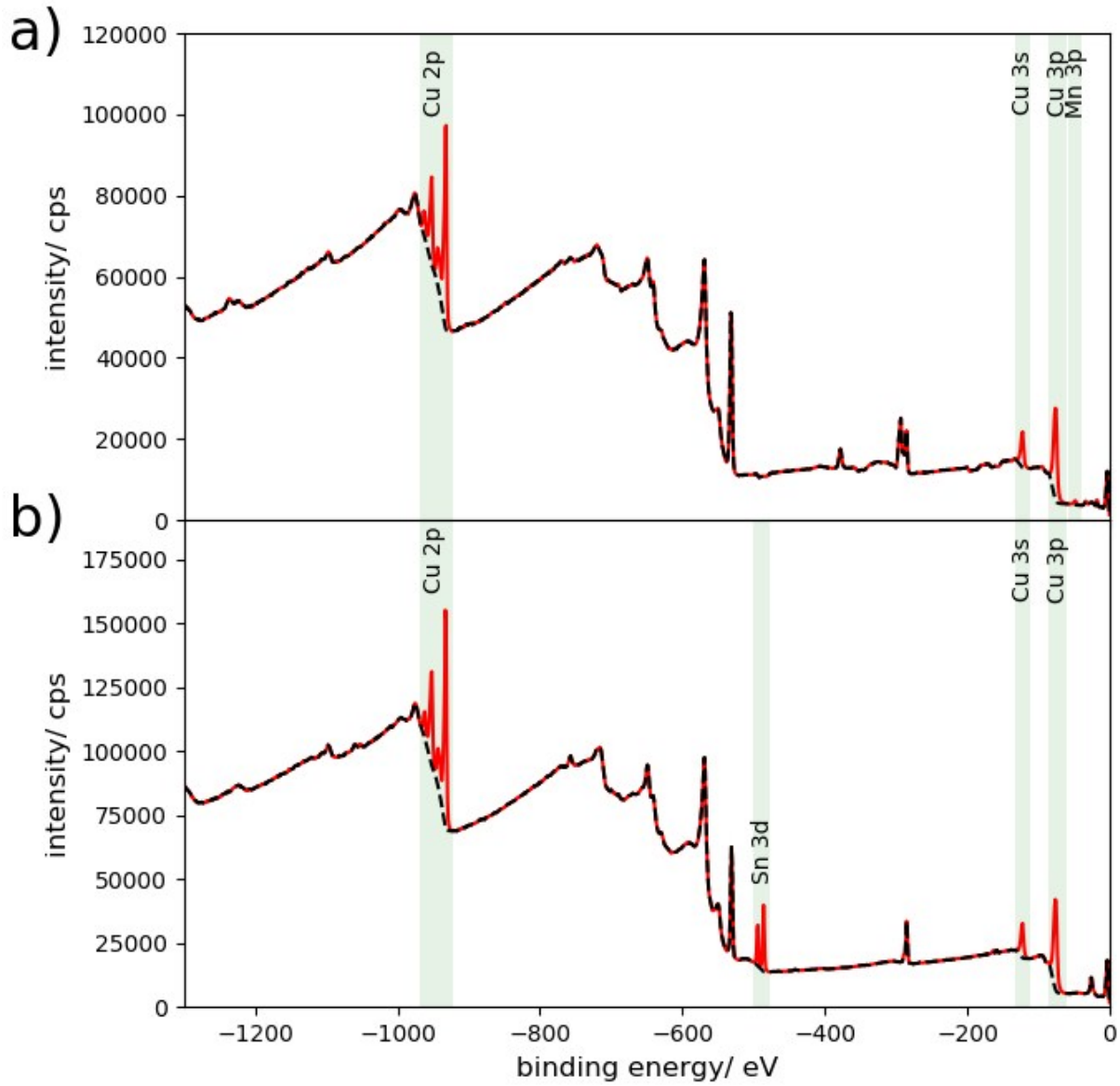

Figure S19. XPS characterization for alloys a) CuMn and b) CuSn. The dashed black line indicates the intensity background which was subtracted for concentration quantification by CasaXPS. CuMn was analyzed by using (Cu 2p + Mn 3p), (Cu 3s + Mn 3p), and (Cu 3p + Mn 3p) and the Mn concentration was calculated to be 14.65 ± 1.78, 11.08 ± 1.38, and 11.37 ± 1.36 %, respectively. CuSn was analyzed by using (Cu 2p + Sn 3d), (Cu 3s + Sn 3d), and (Cu 3p + Sn 3d) and the Sn concentration was calculated to be 14.65 ± 0.92, 11.08 ± 0.71, and 11.37 ± 0.78 %, respectively.

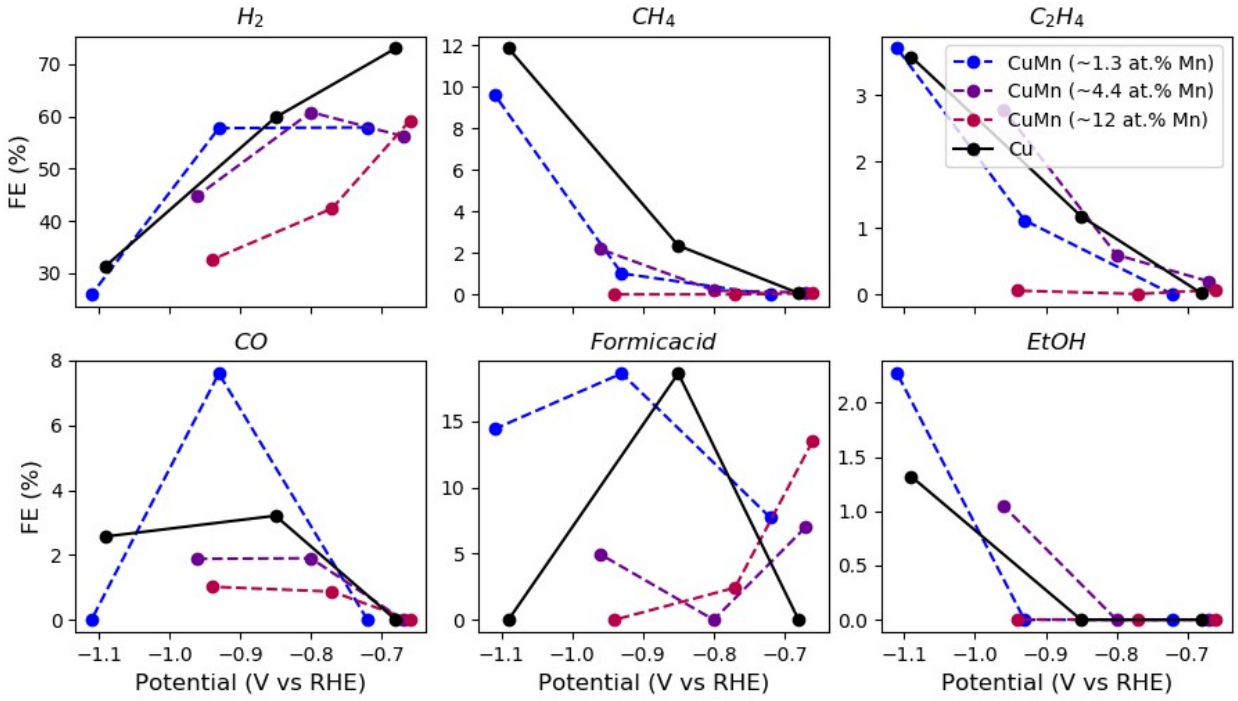

Figure S20. Product distribution of Cu-Mn including liquid product analyzed by ANEC. Note that Mn concentration indicated here is nominal and may vary up to 2 at. % between the tests by ECMS and ANEC due to the location difference on binary plate library

References:

(1) Lai, Y.; Jones, R. J.; Wang, Y.; Zhou, L.; Gregoire, J. M. Scanning Electrochemical Flow Cell with Online Mass Spectroscopy for Accelerated Screening of Carbon Dioxide Reduction Electrocatalysts. *ACS combinatorial science* **2019**.

(2) Jones, R. J. R.; Wang, Y.; Lai, Y.; Shinde, A.; Gregoire, J. M. Reactor Design and Integration with Product Detection to Accelerate Screening of Electrocatalysts for Carbon Dioxide Reduction. *Review of Scientific Instruments* **2018**, *89* (12), 124102. https://doi.org/10.1063/1.5049704.

(3) Gregoire, J. M.; Van Campen, D. G.; Miller, C. E.; Jones, R. J. R.; Suram, S. K.; Mehta, A. High-Throughput Synchrotron X-Ray Diffraction for Combinatorial Phase Mapping. *Journal of Synchrotron Radiation* **2014**, *21* (6), 1262–1268. https://doi.org/10.1107/S1600577514016488.